Structures 41 (2022) 1061–1076

Contents lists available at ScienceDirect

Structures

journal homepage: www.elsevier.com/locate/structures

Regional sustainable development impact through sustainable bridge optimization

Zhi Wu Zhou *, Julián Alcalá, Víctor Yepes

Institute of Concrete Science and Technology (ICITECH), Universitat Politècnica de València, 46022 València, Spain

ARTICLE INFO

Keywords:
Construction
Algorithm program
Structure
Topology
LCA
SIA

ABSTRACT

This paper describes a regional optimal model curve equation to measure and calculate sustainable development assessment impact data related to infrastructure construction in any world region. The article uses a literature review and a case study as research methods—the literature review analyses the importance, practical significance, and current research status of this field. The case study application establishes a scientific algorithm program and a three-dimensional structural topology optimization interactive environment research model. The optimality of the influence equation curve and the sustainable development influence curve of China's large-scale cable-stayed bridges and regional infrastructure is analysed. This research will fill a gap by solving construction industries' tedious and complicated work and sustainable development assessment. Simultaneously, it will provide a theoretical basis and scientific calculation methods for governments and countries to formulate relevant laws and regulations and study regional climate effects.

1. Introduction

The United Nations predicts that 68% of the global population will live in cities by 2050. Infrastructure construction will grow rapidly under the pressure of accelerating processes of urbanization [1]. This intensive development and the use of limited fossil resources will occur together with various impacts on the environment. Reducing fossil fuel consumption and controlling carbon (CO_2) emissions are now common challenges worldwide. The material footprint of global consumption is directly attributed to construction engineering and the use of sand, clay, cement, and stone [2]. The energy consumed by the construction industry accounts for 30–40% of greenhouse gas emissions from the total energy consumption. Reducing greenhouse gas emissions from the construction industry is crucial to addressing climate change [3]. The future development trend must focus on how to effectively reduce the energy and material consumption as well as to develop a sustainable, green, and smart construction industry [4].

The study aims to use several types of scientific research software to analyze the factors that affect the sustainable development of bridge construction in different regions of the world. The environmental, economic, and social relations between the bridge-construction industry and regional development were revealed by establishing a scientific algorithm and studying the three-dimensional (3D) structure topology optimization (TO) model.

The present research contributes to innovation in the field through six points:

1. The clustering statistics method was used to comprehensively analyze the global status of published results in related fields, and which revealed the impact of this research field through assessment and analysis.
2. The comprehensive application of several scientific software packages improves the accuracy and scientific caliber of the calculation process and data quality.
3. A 3D physical model was established to analyze the sustainable development and optimisation process of the construction of bridges, which clearly showed all the details related to the optimisation assessment of the bridge components.
4. The assessment conclusions are systematized through a scientific algorithm program based on the research achievements and recent data, which assesses regional sustainable development, and further promotes the practicability and universality of the research achievements.
5. This study has set a research foundation for follow-up studies on the sustainable development of the national and global regional

* Corresponding author.
E-mail address: zhizh2@doctor.upv.es (Z.W. Zhou).

https://doi.org/10.1016/j.istruc.2022.05.047
Received 1 February 2022; Received in revised form 11 May 2022; Accepted 11 May 2022

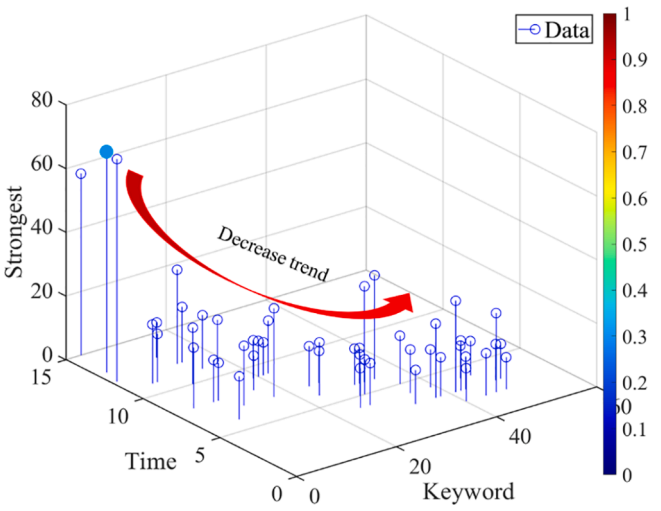

Fig. 1. 'Bridge optimal design' cluster view.

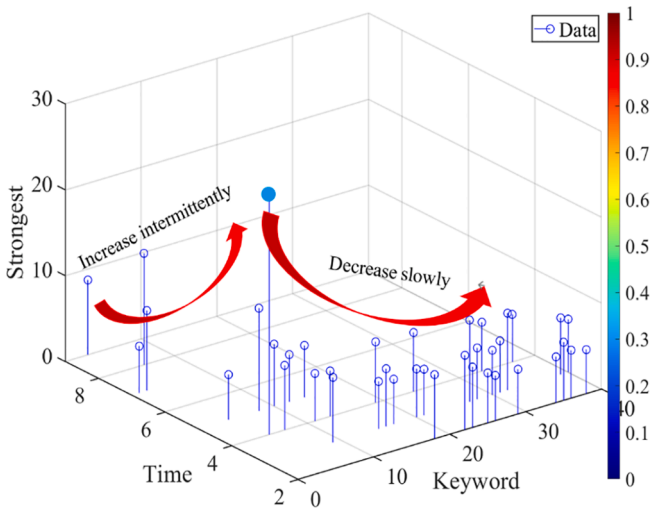

Fig. 2. 'Bridge regional keyword cluster view.

construction industry and highlighted the need for research into global construction and its climate impact.

6. The sustainable development assessment equation established is suitable for infrastructure construction and sustainable development assessment; it can measure the impact data of countries around the world on sustainable development after infrastructure construction.

This present research consists of six parts. In part one, the influence of the current global construction industry is briefly described. Part two includes the literature review and analyzes global sustainable development related to the research topic. In part three, the methodology is described as related to the three major models of the research. In part four, the results, case analysis and model application are discussed. Part five highlights the analysis procedure of the research topic and scientific calculation of the research objective. In part six the conclusions are summarized through the key points of this research and a future research direction is offered.

2. Literature review

For this research the authors carried out an extensive investigation and conducted cluster analysis on related articles. Scopus was used as the search database [5], and the cluster analysis was conducted using CiteSpace software. In the cluster analysis, the frequency (co-word) of two keywords in the same article was obtained, and closely related keywords were joined together to form a cluster (the most influential seed keywords were used to form a cluster first) with the clustering statistics method. Secondly, a new cluster was formed from the seed keywords and adjacent keywords to determine priorities [6].

2.1. Regional economy and natural climate change

The United Nations Framework Convention on Climate Change (UNFCCC) defines climate change as "a change of climate which is attributed directly or indirectly to human activity that alters the composition of the global atmosphere and which is in addition to natural climate variability; observed over comparable periods" [7].

The economic impact of CO_2 changes with the damage function and discount rate. The average additional investment in energy from 2016 to 2050 is about 830 billion USD/year, and the total investment is 1.46 trillion ~ 3.51 trillion USD (for a rise in global temperature <1.5 ℃, compared to 2010) [8]. Regional energy consumption continues to grow with the development of the economy, which has a long-term impact on climate change.

Some 2211 related articles were retrieved and subjected to a cluster analysis from 2000 to 2021(Fig. 2). The cluster analysis revealed that the peak period of research period was from 2000 to 2004, and the research keywords included climate change, environmental protection, and sustainable development. However, the number of research articles decreased after 2014.

2.2. Bridge optimal design

Structural engineers aim to find efficient and economical structural materials both to meet the structural load and to improve performance [9]. For the present study, research progress was identified using the keyword expression "bridge optimal design". In all, 6703 related articles were retrieved from 2000 to 2021 (Fig. 1).

The articles, based on the cluster analysis, were published mostly from 2000 to 2004, and the research hotspot focused on bridge, optimization, and power converter. Then, it entered a low ebb stage. A short growth period occurred from 2008 to 2010, and then it increased slowly. The clustering figure shows a research hotspot around converter > maintenance > cable stayed bridge. The cluster analysis in section 2.3 revealed that studies have focused on bridges in recent years.

2.3. Topology optimisation

Topology optimisation (TO) is a method to find the best design scheme at the conceptual design stage of engineering products, including homogenization methods, solid isotropic material with penalization [10], as well as evolutionary structure and level-set methods. Structure is affected by uncertain factors, such as loading, material properties, geometric perturbation [11], and boundary conditions and model establishment. TO is roughly divided into three types of questions, namely reliability-based topology, robust topology, and equivalent topology [12].

TO can also be divided into discrete structures and continuous structures. After >40 years, development is still limited to the component level and simple working conditions, while the complex structural components and systems face many challenges [13]. 3-D TO results can show the optimal topology shape of each structural component more intuitively and may provide more inspirational conceptual design solutions for designers [14].

A review of the literature highlights the importance and practical significance of this research, which is to develop new research ideas and assessment methods for sustainable development of the construction industry.

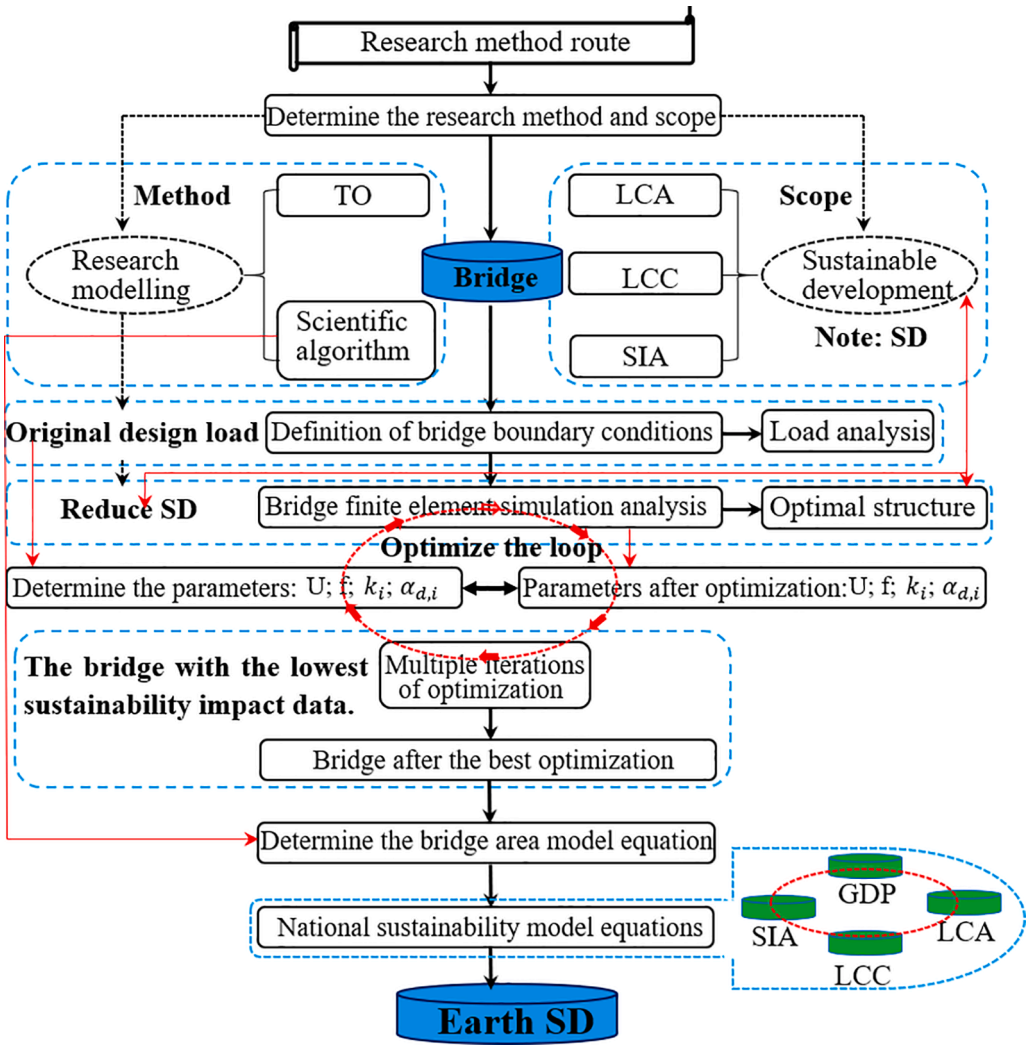

Fig. 3. Schematic of the research process (GDP: Gross Domestic Product).

3. Methodology

The following bases are established to improve the systematization and practicability of the present research, as well as to clarify the research route and method (Fig. 3).

1. This present research analysed the solid structure of bridges and conducted 3D solid modeling using Abaqus software to eliminate the replacement defects of structural components (shell, wire, and point replacement), Utilizing the shell element to perform the 3D domain discretization. The parts were prone to high distortion and a zero-energy model, which caused adverse effects, such as a checkerboard in the TO. Deng and To [15] established the ground structure method model based on projection and found it was only suitable for slender beams, columns, and other components using linear element optimisation. Model failure and local instability were likely to occur during the optimisation period, leading to overall instability [16].

2. Bridges are continuum homogenization structures, and solid isotropic material with penalization (SIMP) is used as the standard TO research method, which is the most successful, the most popular and the most stable shape discrete strategy [17,18].

3. In accordance with the bridge system design research, the Robust TO design is conducted under the condition of fixed static load, but the uncertainty and unstable loads are not considered.

4. In the process of TO research, all the main components of the bridge structure are analysed to avoid the absence of the main components and the reduction in the structure's stability and aseismic design performance [19].

5. This article only analyses the two stages of design and material manufacturers in the sustainable impact analysis. The data research uses the same database as the research literature published by Zhou et al. [20] to ensure the accuracy and completeness of the research system.

6. The primary materials of the case bridge are reinforced concrete, steel strand, pipe materials, and other auxiliary small and sporadic materials. Various materials were selected for TO analysis.

7. The research spanned multiple systems, with massive data and high discreteness and inhomogeneity. To accurately quantify and optimize the weight of each indicator, the introduced parameters and uncertainty factors were all analysed by the software mentioned above, a calculation program was compiled, and judgment based on manual experience was forbidden.

8. The research software includes Citespace 5.7.R5 (for cluster analysis of published articles); Abaqus/CAE6.14-1 (finite elements and analysis of bridge structure) [21]; OpenLCA1.10.1, OpenLCA1.10.3 (assessment and analysis of bridge sustainability); MATLAB R2020B (scientific drawing, calculation fitting and approaching analysis); Relational database: Ecoinvent; MatWeb; Bedec; Product Social Impact Life Cycle Assessment (PSILCA) and Social Hotspots Database (SHDB) [20,22].

3.1. TO modelling

3.1.1. Multi-material structure TO

Optimisation principles: In the finite element fixed domain, the minimum objective function is determined by identifying the solid matter or gap composition of each element; the discrete variables are replaced by continuous variables, and the iterative method and the final interpolation function are determined using the compensation method (applicable to the linear static finite elements and isotropic material analysis) [23]. Optimisation methods: In various materials TO, the composite materials are selected in each subdomain, and the flexible material distribution and independent constitutive relationship are established to avoid the most adverse iteration combinations [24].

3.1.2. Multi-material finite element TO model [25,26]

$$\text{TO model equation}: \begin{cases} Min(\rho,\varphi) = \sum_{i=1}^{n} \Theta_i(\rho_i,\varphi_i) \\ 0 < \rho_i^L \leqslant \rho_i \leqslant \rho_i^U = 1 \\ 0 < \varphi_i^L \leqslant \varphi_i \leqslant \varphi_i^U = 1 \end{cases} \tag{1}$$

θ_i is the response sensitivity weight of the objective function; ρ_i is the element design density vector; φ_i is the element design volume vector; n is total number of finite elements.

For the sensitivity objective function, the following equation is used:

$$\alpha_{d,i} = \sum_{i=1}^{n}\sum_{j=1}^{m} \lambda_{jk} \left| \left\{u_i^j\right\}^T [k_i] \left\{u^i\right\}_k \right| \tag{2}$$

where n and m are the numbers of load groups and displacement constraint groups, respectively; λ_{jk} is the weighted parameters; $\{u^i\}_k$ is the displacement vector of the ith element; $\left\{u_i^j\right\}$ is the displacement vector of the j^{th} element.

For the inner stress, displacement, mutual transfer of energy and robustness of the structure under the static load, eq. (2) is further optimized to enable the structure to achieve convergence and balance.

$$\sum_i^j \alpha = \sum_{i=1}^{n}\sum_{j=1}^{m} \lambda_k \left[k_i^j\right] \left[S_i^j\right] \left[D_i^j\right] \left[E_I^J\right] \tag{3}$$

$\sum_i^j \alpha$ are sensitivity parameters; $\sum_{i=1}^{n}\sum_{j=1}^{m}\lambda_k$ are weighted parameters of the structure under the constraints of load and displacement of n and m groups; $\left[k_i^j\right]$ are stiffness matrix (k refers to the ability of an elastomer to resist the deformation stretch; $K = P/\delta$. P is the constant force acting on the structure; δ is the deformation caused by the force); $\left[S_i^j\right]$ are elasticity matrix of the structure (the high deformability of elastomer and the difference of the stress field between the elastic source and structure caused by deformation.) [27]; $\left[D_i^j\right]$ are displacement matrix of the structure; $\left[E_I^J\right]$ are energy matrix of the structure.

3.2. Sustainability modelling

Sustainable development includes three associated pillars, namely environment-Life cycle assessment (LCA), economy-Life cycle cost (LCC) and Society impact assessment (SIA) [28]. Ballet et al. proposed the new framework and indicator scope of the social impact of sustainable development:

Level I indicators: Social pillars and social sustainability.

Level II indicators: Social cohesion, level of social equity and so on [29].

Level III indicators: Social justice, community well-being, human scale development and so on [20].

3.2.1. Environment

ISO14044:2006 defined the assessment scope for LCA requirements and criteria [30]. LCA is carried out based on the nine factors defined by the software, and the modelling method focuses on midpoint modelling. When there are environmental impacts between stages, the endpoint modelling is used to set the weights [31,32].

$$\sum_{t=Start}^{t=Finshed} E_s = \left[\sum_{t=Start}^{t=Finshed} E_{summary}(\overline{s},t_d)\right] \Big/ (1 \pm \gamma_s\%) + \left[\sum_{t=Start}^{t=Finshed} E_{summary}(\overline{m},t_m)\right] \Big/ (1 \pm \gamma_m\%) \tag{4}$$

$\sum_{t=Start}^{t=Finshed} E_s$ is the environmental impact of the two stages related to design and material manufacturing (kg); $\sum_{t=Start}^{t=Finshed} E_{summary}(\overline{s},t_d)$ is the environmental impact during the design stage (kg); $\sum_{t=Start}^{t=Finshed} E_{summary}(\overline{m},t_m)$ is the environmental impact in the material manufacturing stage (kg); γ_s% and γ_m% are the weight coefficients influencing the two stages (%).

3.2.2. Economic

The reason for the substantial increase in global resource extraction is the growth in living standards and increased investment in infrastructure by developing countries and transition countries [33], where rapid urbanization is further aggravating the damage to the natural environment and global climate [34].The demand for resources, including biomass, fossil fuels, metals, and minerals, is expected to double from 2015 to 2060 [35]. While the investment in circular economy systems, the improvement of operational efficiency, and cost-saving, the reduction in wastes and emissions, for example, have been included in national economic policies [36].

Elmagrhi et al. [37] defined variables and econometric models to study the relationship between environmental performance, national policies, and management performance. Shahab et al. [38] analysed the sustainable development and ecological performance impact using the least squares dummy variables panel regression technique. Lu et al. [39] proposed the vector error correction model to study the relationship between corporate social responsibility and corporate financial performance and used the Fisher-Johansen test to coordinate, track and test the model.

$$Ln\text{REV}_{it} = \beta_0 + \text{CSR}_{it} \times \beta_i + C_{it} \times \gamma + \mu_{it} \tag{5}$$

$$C_{it}\gamma = DE_{it}\gamma_1 + \text{FirmSize}_{it}\gamma_2 + \sum \text{NationLevel}_{ij}\gamma_{3j} + \text{Industry}\gamma_4 + \text{TimeEffect}(08)\gamma_5 + \text{TimeEffect}(09)\gamma_6 \tag{6}$$

LnREV refers to the natural logarithm of revenue; i refers to a single company; t is time; LnREV$_{it}$ refers to the dependent variables and the natural logarithm of income; CSR$_{it}$ is the independent variable; C_{it} is the control variable; β_i and γ are two variation coefficients; β_0 is a constant term; μ_{it} is the error term.

Zhou et al. [20] studied the sustainability of bridges in the full life cycle, which provided the modelling basis for the present research. In accordance with Formulas (5) and (6) and the research by Zhou et al., the economic cost and sustainable development model are established as follows:

$$\sum_{t=Design}^{t=Materialmanufacturing} C_T = \left[\frac{\text{C}_{\text{Design}}(\overline{x},t_d) + C_{\text{Material}}(\overline{y},t_m)}{(1+r)^t}\right] + C_d \tag{7}$$

$\sum_{t=Design}^{t=Materialmanufacturing} C_T$ is the social impact produced during the design and material manufacturing stage (Chinese Yuan: CNY); $\text{C}_{\text{Design}}(\overline{x},t_d)$ is

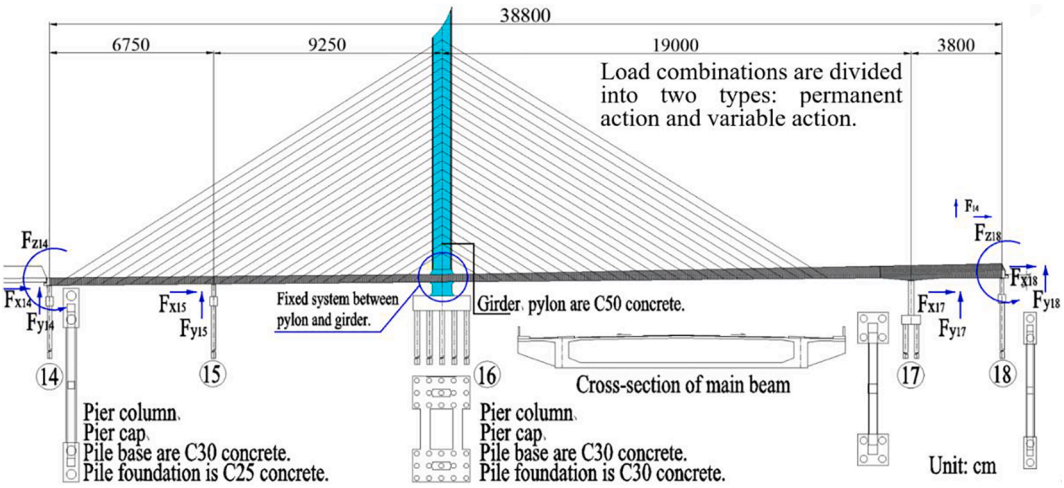

Fig. 4. The related parameters of STB bridge.

the design cost (CNY); $C_{Material}(\overline{y}, t_m)$ is the materials cost (CNY); r is the discount rate (%); C_d is the actual direct costs (CNY).

3.2.3. Social

The International Finance Corporation's Performance Standards on Social & Environmental Sustainability (IFC, 2012a) has become the globally accepted guideline for managing environmental and social risks [40]. The standards formulated a total of eight assessment criteria: Assessment and management of ecological and social risks and impacts, labor and working conditions, resource efficiency and pollution control, community health, safety, and public security, land acquisition and involuntary relocation, biodiversity protection and sustainable management of biological natural resources, aboriginal and culture heritage. However, there is no aboriginal consideration within the case research community; no cultural heritage is left or is newly built in the case construction area, so these are not considered in the research [20,41]. The remaining five assessment criteria are used as the social impact research parameters.

$$S^{T=\text{Finished material}}_{T=\text{Start design}} = S_1 + S_2 + \cdots\cdots + S_n \tag{8}$$

$S^{T=\text{Finished material}}_{T=\text{Start design}}$ refers to the environmental impact caused by the two stages of design and material manufacturing (Both PSILCA and SHDB databases are inspired by UNEP(The United Nations Environment Programmer) SETAC(The Society of Environmental Toxicology and Chemistry) guidelines and use "Med risk hour" to quantify social impact indicators [42]; $S_1 \cdots S_n$ refers to different types of social impact data (Med risk hours).

3.3. Scientific algorithm

The MATLAB program is completed with a high-level programming language, using the rigorous scientific and extensive predefined library functions. The computational simulation and research process are done with the available structural analysis program [43].

3.3.1. Curve fitting

Fitting principle: The least-squares method is an advanced mathematical optimisation technique that minimizes the square error and searches for the best function match for the data. After the curve fitting, the trend of sustainability influence is predicted, and the diversity and convergence of the optimisation parameters will be properly handled to prevent optimal local phenomenon. Programmed algorithm finished.

3.3.2. Multi-factor approximation

Approaching principle: To determine if the main effect and the mutual effect of multiple factors are obvious, it is necessary to establish the mean value and conduct the normalization processing by analyzing the influencing factors to achieve the best goodness of fit and the selection of the influence equation.

It is assumed that $p(x)$ is the polynomial function $p(x)=a_m x^m + a_{m-1}x^{m-1} + \cdots a_1 x + a_0$, and $\sum_{i=1}^{N}[p(x_i) - y_i]^2$ has the minimum value, then the $p(x)$ is the primitive function, $y = f(x)$ approximation function, and the cftool function shall be used to conduct the approaching analysis of multiple factors. Programmed algorithm finished.

4. Results

4.1. Case description

The case cable-stayed bridge, named South Tai Hu Lake Bridge (STB), is located on the urban expressway in Huzhou, China. Based on the city-Level A load design, the vehicle speed is 60 km/h. The bridge is an H-shaped cable-stayed bridge with a single tower and double cable plane concrete. The main bridge span is 160 m + 190 m + 38m, with a total length of 388 m. The main girder is 3.055 m in height and 40.5 m in width and is composed of central ribs, bridge decks, and diaphragms. The central rib is 2.7 m in size and 1.7 m in width. The standard longitudinal spacing of the diaphragm is 6 m, with a calculation span of 35 m. The thickness of the diaphragma and the bridge deck is 28 cm. The bridge includes a central tower (including the main pier and girder of Concrete 50), cap beams, columns, bearing platforms, collar beams, guard rails, bored piles (Concrete 30), and stay cables (OVM250-55 strand stay cable). There are 24 pairs of stay cables on each side (as show in Fig. 4).

4.2. Load analysis

In accordance with the provisions of China's JTG D60-2015, the load distribution coefficient of the transverse lanes of *STB* is 1.00 (two lanes); the longitudinal reduction coefficient is 0.97 (150 m < design span < 400 m) L_0 [44].

$$\sum_{s=Design}^{Types} F_b = \sum G_{\text{Structure}} + F_{\text{Preload}} + \sum F_{\text{Car load}} + F_{\text{Car impact}} + F_{\text{Car braking force}} + F_{\text{Crowd load}} \tag{9}$$

$\sum G_{\text{Structure}}$ refers to the structure gravity (kN); F_{Preload} is the preload force (kN); $F_{\text{Car load}}$ is the car load (even load + concentrated load + vehicle load (kN)); $F_{\text{Car impact}}$ is the car impact force (kN); $F_{\text{Car braking force}}$ is the car

Table 1
Main engineering quantities data and load calculation data of STB.

Location	Pylon (m^3)	Ancillary structure (m^3)		
Name	Pile foundation	Asphalt concrete	Guardrail	Stay cable
STB	3,057.94	616.92	371.82	12,096.46
Pressure (N/m^2)	78,714.00	1,611,329 (153-Stay Cable)		

Location	Lower structure (m^3)				
Name	Pile foundation	Pile platform	Pier column	Pier cap	Girder
STB	10,910.60	5,939.60	276.63	230.49	15,374.80
Pressure (N/m^2)	Within the 1,611,329 data range				26,554.00
Pressure (N/m^2)	$F_{\text{Car load}}$ = 34.33; $F_{\text{Car impact}}$=15.45; $F_{\text{Car braking force}}$=2.1; $F_{\text{Crowd load}}$ = 2.5; $F_{\text{Guardrail}}$=1.0.				

Note: the cable-stayed bridge is designed according to the statically indeterminate structure, and the preload should be considered a permanent load to calculate the prestress loss. The pre-tightening force is mainly distributed on the steel bars of the main beam and the central tower.

braking force (kN); $F_{\text{Lane load}}$ is the lane load (kN); $F_{\text{Vehicle load}}$ is the vehicle load (kN/m^2); $F_{\text{Crowd load}}$ is the crowd load (kN/m^2).

4.3. STB finite element analysis

STB is assembled based on the distributed components (Fig. 4). Six groups of components are divided into 630,148 sets of unit grids. Given the long girder and stay cable in the Z direction, the grid set is divided into 0.5, and another component grid is 1. The types of materials are listed in Table 1, and the values of mass density, Young's modulus, and Poisson's ratio of C30 and C50 are 2316 kg/m3 and 2332 kg/m3; 28,850 × 10^6 Pa and 33,180 × 10^6 Pa; 0.233 and 0.254, respectively. The values of the stay cable are 65.23 kg/m^3, 1,190 × 10^6 Pa and 0.3 (the values are selected from the Ecoinvent database).

Fig. 5 shows the final deformation state of STB after the stress, and the maximum stress is 81,347 sets. The stress is 130,000,456 Pa. The maximum displacement is at the 4,432 sets position of #16-#17 girder, with the displacement of 1.866 m.

4.3.1. Girder

Fig. 6a indicates that 42 sets of displacement and stress data were detected on the beam surface of the main girder within 15 frames. The top five sets of the stress are 81,347 (130,000,456 Pa) > 88672 (102,859,592 Pa) > 81343(89,389,608 Pa) > 81435(88,824,336 Pa) > 88243(88,636,112 Pa), (The top five sets of strain data of all components shall be noted). The stress points are located above the left cushion stone in ①, ②, in Fig. 5, the remaining 3 points are all above the cushion stone on both sides of pier #17 ③. The top five sets of the displacement are 81,374 (1.853 m) > 100959 (1.833 m) > 100304(1.832 m) > 87777 (1.785 m) > 81601(1.782 m), which are located in ①, ④, ⑤, ⑥, ⑦ in Fig. 5.

It was found that the displacement of four of the largest five sets is not at the place where the maximum stress is applied. The reasons are as follows: after STB bears the load, the effective transverse and longitudinal confining stress along with the stress transfer on pier #17 prevents the deformation of the main girder components at this position, but stress diffusion occurs along the lateral, longitudinal and vertical directions of the pier column, which causes the new stress distribution and a secondary transfer of stress in the constrained region. This is consistent with the experimental results of Li et al. [45,46].

As shown in Fig. 6b, 42 sets of energy and strain data synchronized with Fig. 5 on the main girder plate surface were detected, with the energy ranking: 88672(189,668.5938 J) > 81343(132,429.125 J) > 81435(127,804.6 J) > 88243(127,633.1 J) > 88476(115,846 J). The position is the same as the stress distribution position. Strain ranking is given as 101130(0.001065 m) > 101138(0.001064 m) > 101189 (0.001024 m) > 81601(0.001017 m) > 81374(0.0009242 m); The first three sets are located in ⑧, ⑨, and ⑩ in the girder (Fig. 5); the position of the remaining two points remains unchanged. The above five sets present the maximum deformation of the main girder in this area.

To introduce the decision for parameter redundancy, two or more types of data are combined and then described using an integrated overall model [47].

4.3.2. #14, #15, #17 and #18 piers

As shown in Fig. 7a, #14 pier measures 26 sets of displacement and stress data, with the stress ranking: 515913(22,706,152 Pa) > 516585 (22,378,020 Pa) > 514545(15,981,374 Pa) > 516666(15,254,124 Pa) > 515557(3,904,752.5 Pa); displacement ranking: 75965(0.7736 m) > 26210(0.7681 m) > 19788(0.7655 m) > 93153(0.7550 m) > 26188 (0.7463 m), As shown in Fig. 7b, through the fitting data analysis, in the early stage of loading, the stress tends to increase in a straight line, while in the middle and late stages of loading, the stress is distributed

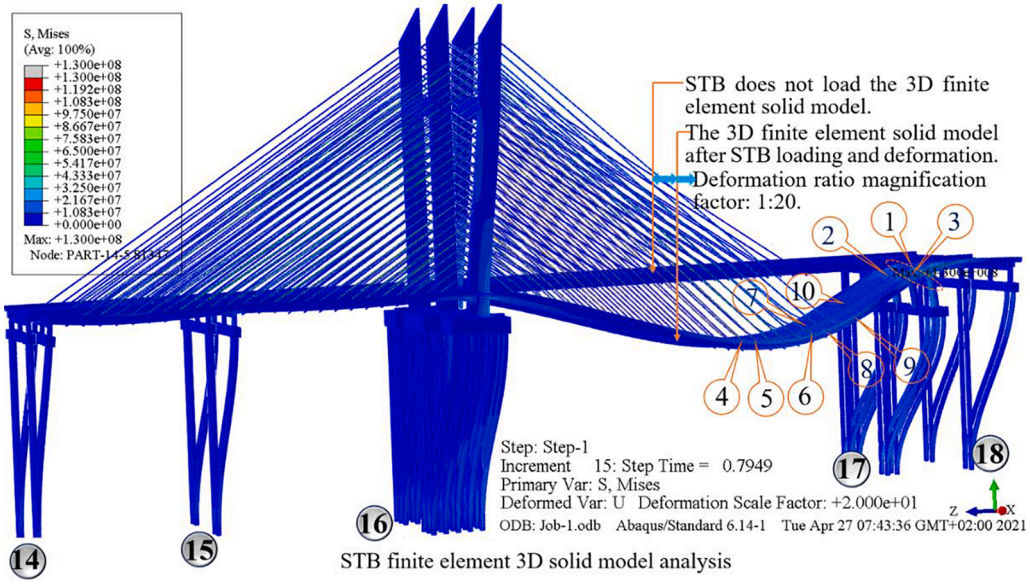

Fig. 5. STB finite element model analysis.

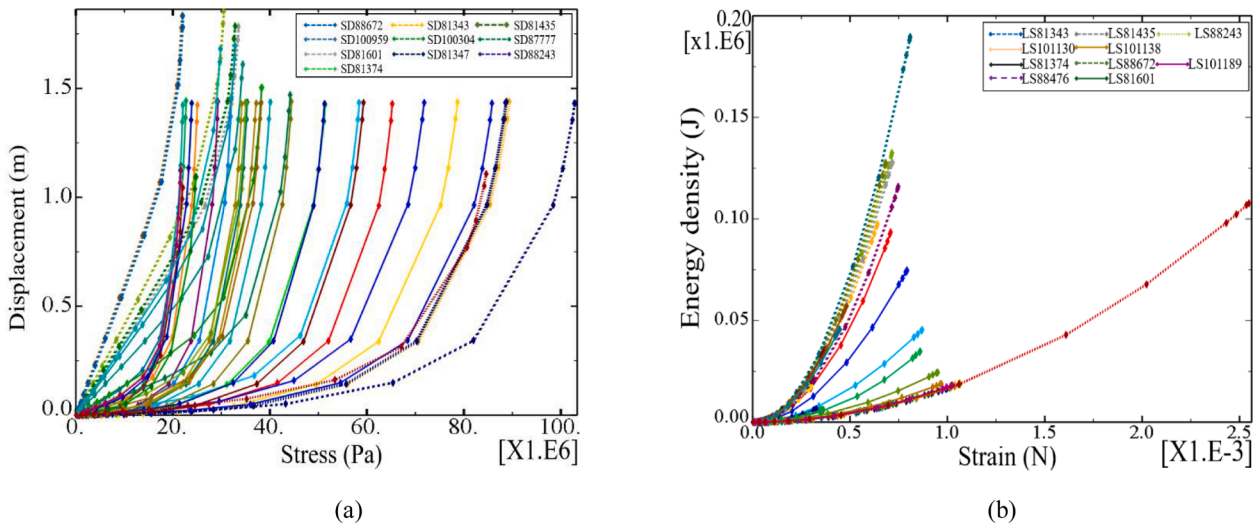

(a) (b)

Fig. 6. Fitting of stress and displacement. Finite element fitting analysis of the girder: (a) Secondary stress distribution; (b) Monitoring area distribution (multiple set points were selected for analysis. The figure frame is limited, and only the first 10 set legends are indicated).

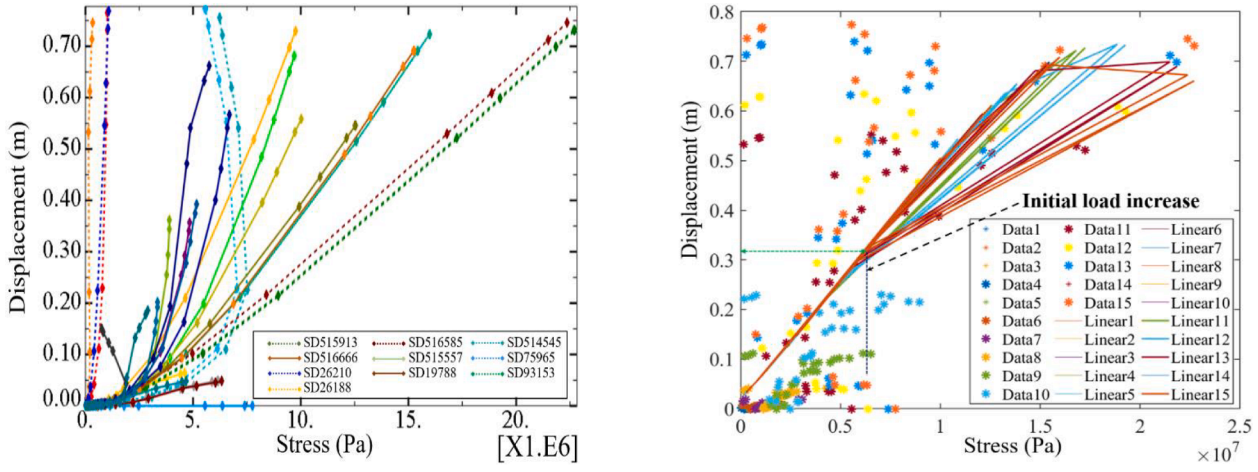

(a) (b)

Fig. 7. Finite element fitting analysis of #14: (a) #14 stress and displacement analysis; (b) #14 fitting of stress and displacement.

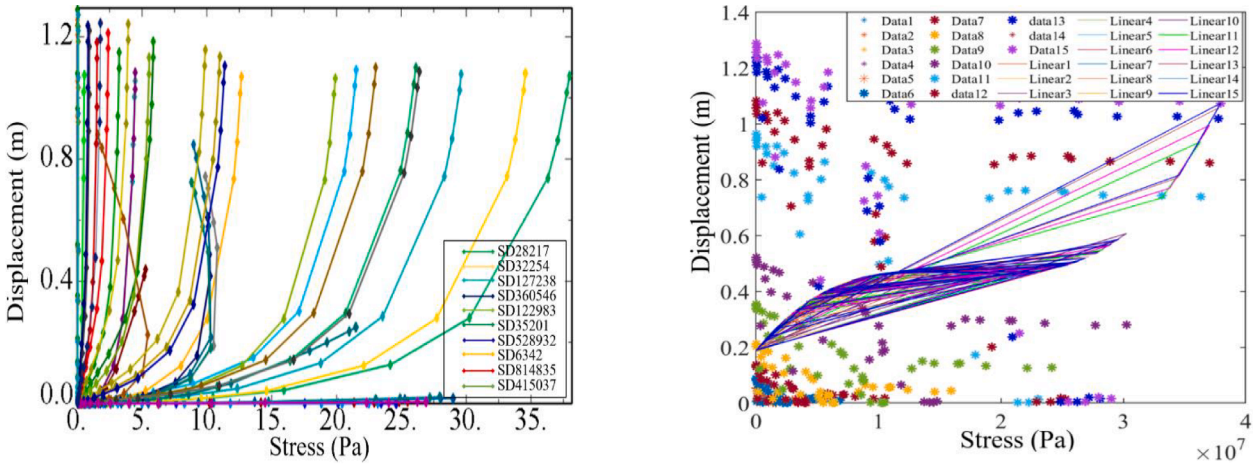

(a) (b)

Fig. 8. Finite element fitting analysis of #16 bridge pylon: (a)#16 stress and displacement analysis; (b)#16 fitting of stress and displacement.

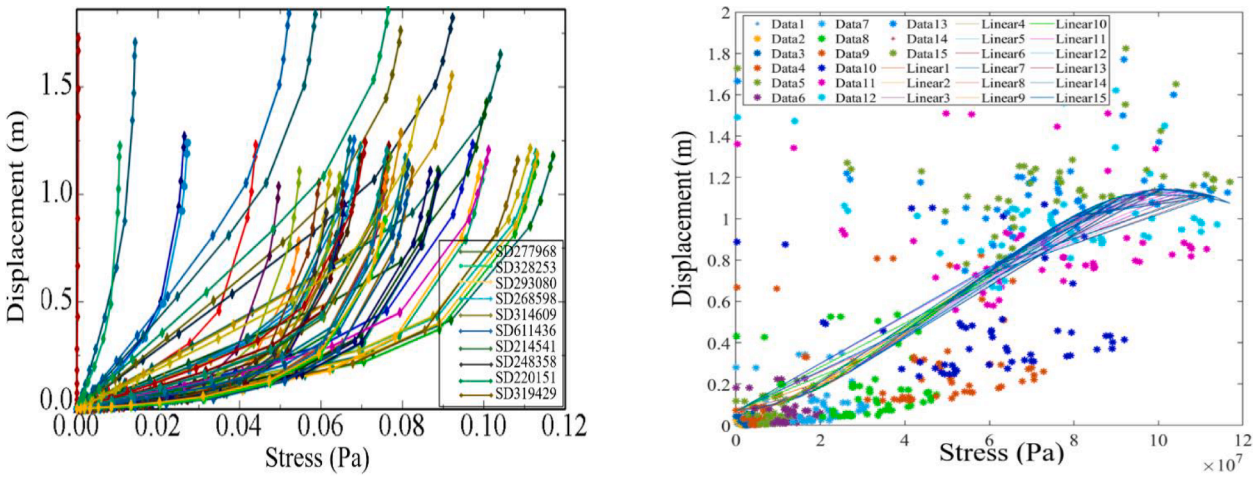

Fig. 9. Stay cable analysis: (a) Stay cable stress and displacement analysis; (b) Stay cable fitting of stress and displacement.

discretely. It is initially thought that there is parameter redundancy in #14, and that the components can be optimized.

As seen in Fig. 7a, b a method analysis can be obtained, #15 pier measures 18 sets of displacement and stress data, with the stress ranking: 517445(13,554,358 Pa) > 519454(12,399,145 Pa) > 518226 (12,115,227 Pa) > 518852(12,163,226 Pa) > 518988(8,401,345 Pa); displacement ranking: 226(0.904 m) > 1942(0.899 m) > 217(0.896 m) > 236(0.889 m) > 725(0.885 m). Through the fitting data analysis, in the overall loading process, the curve increases and tends to be a curve without discrete distribution. It is initially thought that there is no parameter redundancy in #15, and that the components cannot be optimized.

Similar to Fig. 7a, b a method analysis can be obtained, the #17 pier measures 40 sets of displacement and stress data, with the stress ranking: 17,644 (56,986,496 Pa) > 520129 (44,066,036 Pa) > 97837 (37,494,904 Pa) > 521287 (35,395,728 Pa) > 87149 (29,460,000 Pa); displacement ranking: 524,023 (1.463 m) > 524626 (1.462 m) > 32555 (1.461 m) > 42451(1.452 m) > 5152(1.450 m). Through the fitting data analysis, the overall loading process tends to be an increasing curve, but the discrete distribution of the fitting curve is obvious. It is initially thought that there is parameter redundancy, and that the #17 components can be optimized.

Similar to Fig. 7a, b a method analysis can be obtained, #18 pier measures 16 sets of displacement and stress data, with the stress ranking: 42,682 (19,369,772 Pa) > 43400 (14,748,930 Pa) > 42790 (14,268,664 Pa) > 45152 (10,151,770 Pa) > 44828 (9,118,991 Pa); displacement ranking: 5006 (1.503 m) > 5 (1.501 m) > 513719 (1.501 m) > 526746 (1.499 m) > 31(1.492 m). Through the fitting data analysis, in the loading process, the curve tends to increase discretely, and the stress distribution is obvious. It is initially thought that there is parameter redundancy, and that the #18 components can be optimized.

After research and analysis in 4.3.2, it is concluded that #14, #17, and #18 have TO conditions and have redundant structures.

4.3.3. #16 pylon

As shown in Fig. 8a, the #16 pylon measures 42 sets of displacement and stress data, with the stress ranking: 28127(37,963,836 Pa) > 32254 (34,573,160 Pa) > 127238(29,012,396 Pa) > 360546(26,385,628 Pa) > 122983(25,485,788 Pa); displacement ranking: 35201(1.288 m) > 528932(1.273 m) > 6342(1.256 m) > 814835(1.246 m) > 415037 (1.243 m). As shown in Fig. 8b, through the fitting data analysis, in the loading process, the curve presents a wide range of discrete distribution. In the later stage, the dispersion curve deviates from the fitting interval of the original curve. The dispersion curve is distributed in two regions. It is initially thought that there is no parameter redundancy, and that the components cannot be optimized.

4.3.4. Stay cable

As shown in Fig. 9a, the stay cable pier measures 42 sets of displacement and stress data, with the stress ranking:268598 (116,968,440 Pa) > 328253(113,165,800 Pa) > 293080(113,015,920 Pa) > 268598(112,841,672 Pa) > 314609(111,346,136 Pa); displacement ranking: 611436(1.852 m) > 214541(1.843 m) > 248358(1.837 m) > 220151(1.823 m) > 319429(1.761 m). As shown in Fig. 9b, through the fitting data analysis, there is no discrete state in the curve in the whole loading stage, and the stress is distributed stably and discretely in the fitting range. It is preliminarily judged that there is no parameter redundancy, and that the stay cable components cannot be optimized.

4.4. Sensitivity

The stiffness of a reinforced concrete structure is related to the material stress, strain and energy dissipated by unit volume damping, while

Table 2
The selected set numbers.

Location	Set numbers									
Girder	81,347	88,672	81,343	81,435	88,243	88,476	81,374	100,959	100,304	87,777
#14	515,913	516,585	514,545	516,666	515,557	75,965	26,210	19,788	93,153	26,188
#15	517,445	519,454	518,226	518,852	518,988	226	1942	217	236	725
#16	28,127	32,254	127,238	360,546	4859	35,201	528,932	6342	814,835	415,037
#17	17,644	520,129	97,837	87,149	521,287	524,023	524,626	32,555	42,451	5152
#18	42,682	43,400	42,790	45,152	44,828	5006	5	513,719	526,746	31
Stay cable	268,598	328,253	293,080	268,598	314,609	611,436	214,541	248,358	220,151	319,429

Table 3
Constraint conditions for structural TO.

Optimisation constraints	Stress (Pa)		Displacement (m)		Sensitivity	
	Maximum value	Minimum value	Maximum value	Minimum value	Maximum value	Minimum value
#14	22,706,152.000	323,264.344	0.774	0.049	187,994.480	55.949
#17	56,986,496.000	82,736.640	1.462	0.001		
#18	19,369,772.000	2,528.800	1.503	0.357		
STB	130,000,456.000	0.000	1.853	0.000		

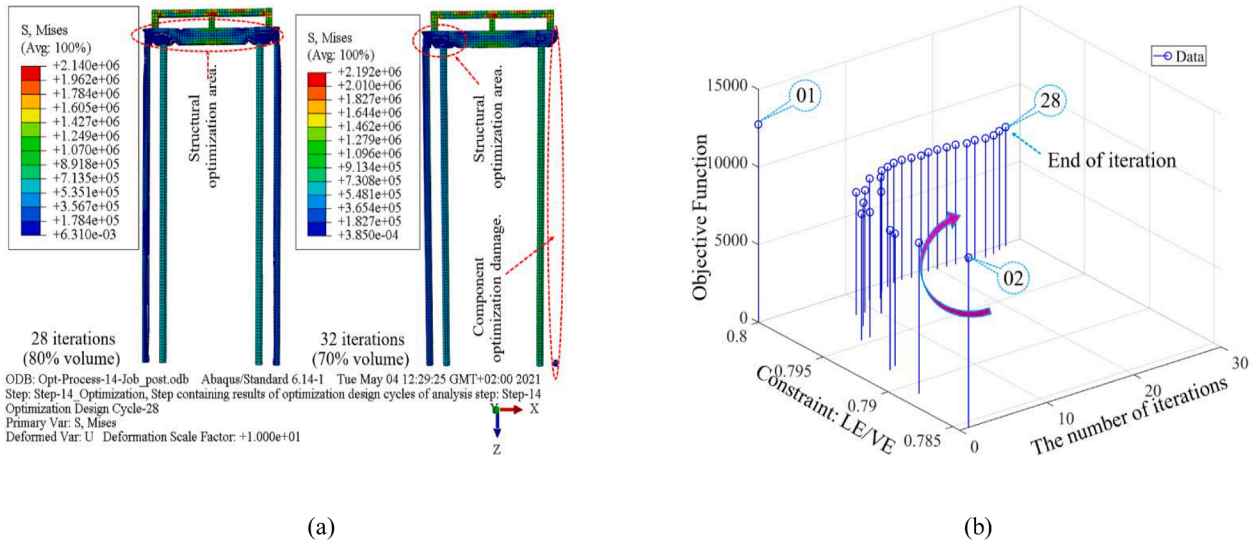

(a) (b)

Fig. 10. #14 cloud map and iterative data after two optimisations: (a) Cloud map analysis; (b) Iterative data.

the strain amplitude and strain rate can define the structural loss of stiffness [48,49]. Ten sets with maximum stress and displacement of each component group were selected for analysis (Table 2).

The STB sensitivity is calculated according to eq. (2) and (3), which are used as the judgment standard for the subsequent TO.

The calculation results are as follows: The values of k_i^j are [0.000924, ……,0.00241]. The values of S_i^j, D_i^j,E_i^j are the stress values of the maximum 10 sets of the structure (Girder, #14, #15, #17 and #18piers, #16pylon, stay cable),S_i^j are [130,000,456,……,88,636,112]; D_i^j are [1.853,……,1.782]; E_i^j are [189,668.59, ……,115,846];The values of λ_k are [0.01,……,0.794,907,808] (the variation-weighted parameters of structures under load and displacement constraints).

After using MATLAB data matrix to calculate the sensitivity parameter range ($\sum_i^j \alpha$ are [1,201.46 8,8.62 55.95 1,025.84 5,178.06 2,745,760.15 87,500.38 151,000.45 2,608.29 1,235.42 26,211.82

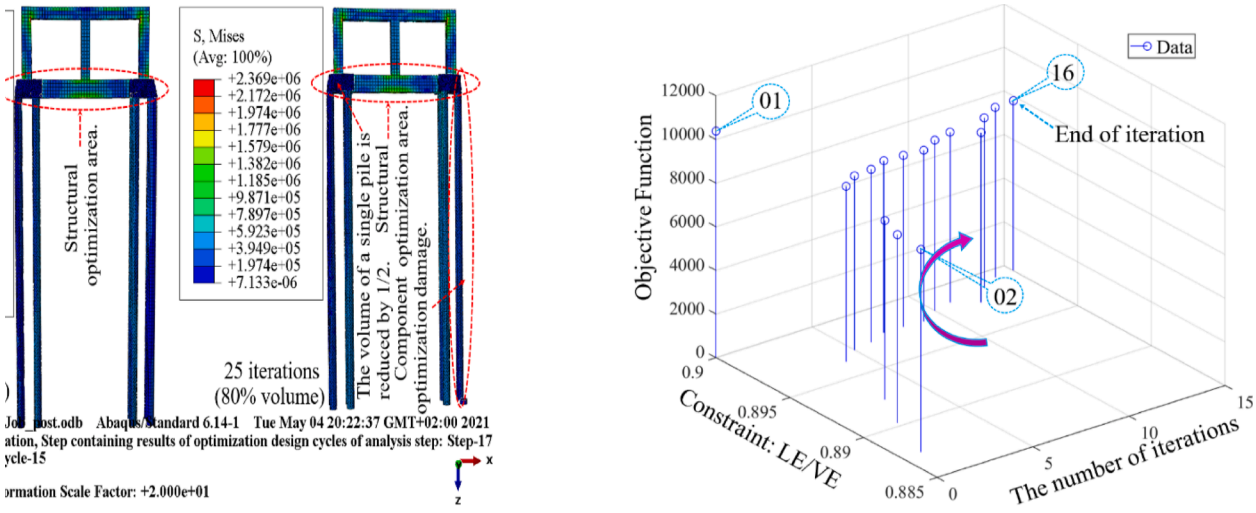

(a) (b)

Fig. 11. #17 cloud map and iterative data after two optimisations: (a) Cloud map analysis; (b) Iterative data.

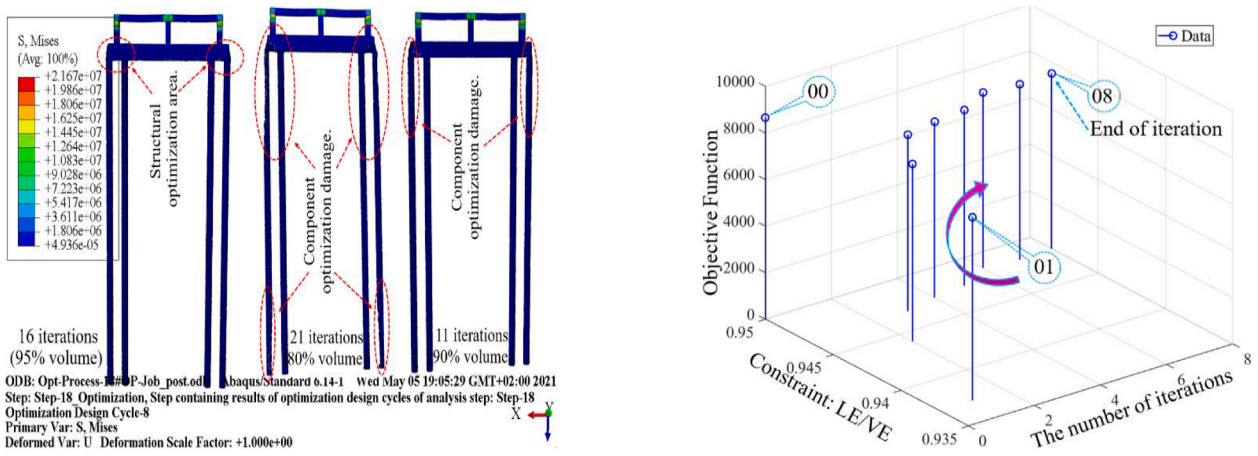

(a) (b)

Fig. 12. #18 cloud map and iterative data after three optimisations: (a) Cloud map analysis; (b) Iterative data.

60,864.63 8,818.59 187,994.48]). $\sum_i^j \alpha$ is also one of the criteria for TO judgment.

4.5. Topology optimization

The conclusion from the analysis according to 4.3 is that girder, #15, #16 and stay cables do not have parameter redundancy, and these components cannot be subjected to TO analysis. #14, #17 and #18 have TO parameter redundancy and can subjected to reloading analysis based on 4.2. Please see the optimisation constraint range in Table 3.

4.5.1. Parts of #14

TO aims to reduce the component volume based on meeting the design conditions, and to optimize the parts, including foundation piles.

As shown in Fig. 10a, #14 is analyzed in two TO processes. The volume was reduced by 20% the first time. After 28 iterations, the volume of the cover beam was reduced. The maximum stress is 2,140,400 Pa and is located at the connection between the cover beam and the middle top collar beam. The maximum displacement is 0.7736 m, and the sensitivity range is 14969.677–53861.4370. The volume was reduced by 30% the second time, and the optimization ended after 32 iterations. The maximum stress is 2,192,000 Pa, and the maximum displacement is 0.0197 m. Observing Fig. 10b in the right cloud image (the second optimization), one pile in the structural pile foundation is missing, and the component is damaged, which does not meet the requirements of 3.0. The second TO fails.

In the structure TO, $\left[k_i^j\right]$ and $\left[E_I^J\right]$ remain as in the original array. The essence of the optimisation is the robust compensation design of the micro-structure, and the whole structure will not be damaged [50].

The values of S_i^j are 1,790,000…, 2,260,000. The values of D_i^j are 0.004167178…,0.019719347.

$\sum_i^j \alpha_{14}$ are 14,969.6775–53,861.4370. The calculation method is the same as in 4.4.

Conclusion: The TO monitored values of #14 pier analysed for the first time fulfilled the conditions listed Table 3 and 3.0, and the volume can be reduced by 20%.

4.5.2. Parts of #17

The TO reduced the volume by 10% the first time (the new volume is 90% of the original volume), and the number of iterations was 16. The maximum stress was 2,413,272 Pa, and the maximum displacement was 0.00363 m. The sensitivity range was 5,037.494–6,775.711. The TO reduced the volume by 20% the second time, and the number of iterations was 25. The maximum stress was 2,369,000 Pa, and the maximum displacement was 0.00397 m. The sensitivity range was 9,795.690–11,453.2705, and the range of the above values met the requirements listed in Table 3. Observing Fig. 11a in the right cloud image (the second optimisation), 1/2 of one pile in the structural pile foundation and one pile on the other side are missing (Fig. 11b), and the component is damaged, which does not meet the requirements of 3.0, and the second TO fails.

The values of S_i^j are 1,840,000…,2,370,000. The values of D_i^j are 0.00154…,0.00692.

$\sum_i^j \alpha_{17}$ are 5,037.494–11,453.2705 . The calculation method is the same as in 4.4.

Conclusion: The TO monitored values of #17 pier the first time met the conditions listed in Table 3 and 3.0, and the volume can be reduced by 10%.

4.5.3. Parts of #18

The TO reduced the volume by 5% the first time, and the number of iterations was 8. The maximum stress was 21,670,000 Pa, and the maximum displacement was 0.00597 m. The sensitivity range was 100702.6873–120703.4437, and the range of the above values met the requirements listed in Table 3. The TO reduce the volume by 10% the second time, and the number of iterations was 11. The maximum stress was 21,650,000 Pa, and the maximum displacement was 0.00621 m. The sensitivity range was 175,598.373–238,794.422, which did not meet the requirements given in Table 3. Observing Fig. 12a in the cloud image, 1/4 of the upper position of two piles in the structural pile foundation is missing, and the component is damaged, which does not meet the requirements of 3.0, and the TO fails. The TO reduce the volume by 20% the third time, and the number of iterations was 21. The maximum stress was 21,580,000 Pa, and the maximum displacement was 0.00639 m. The sensitivity range was 13,143.825–19,360.961. Observing Fig. 12b in the cloud image, 1/2 of two piles in the structural pile foundation on both sides is missing, and the component is damaged. The TO fails. The second and third sets of optimisation data indicated that the number of optimisations is directly proportional to the reduction in the component volume (the topological properties of materials can be found based on this research).

The values of S_i^j are 451,000…,21,300,000. The values of D_i^j are 0.000812…,0.00695.

$\sum_i^j \alpha_{18}$ are 100,702.687–120,703.444 . The calculation method is the same as 4.4.

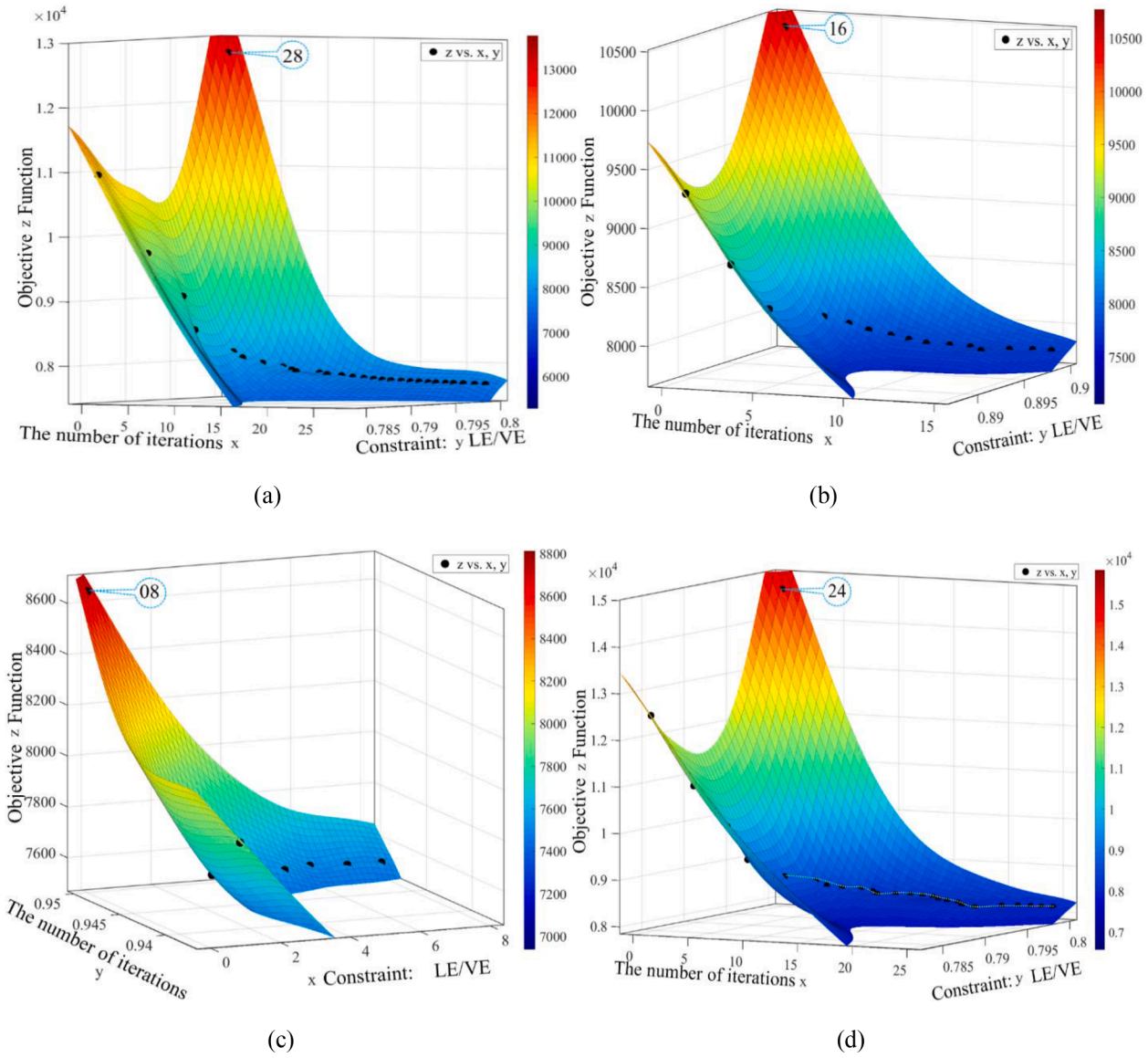

Fig. 13. TO interpolation approximation analysis: (a) #14 TO interpolation approximation analysis (80–90%); (b) #17 TO interpolation approximation analysis (80–90%); (c) #18 TO interpolation approximation analysis (95%); (d) #18 TO interpolation approximation analysis (80%).

Conclusion: The TO monitored values of #18 pier met the conditions given in Table 3 and 3.0 the first time, and the volume can be reduced by 5%.

4.5.4. #14, #17 and #18 interpolation approximation analysis

As shown in Fig. 13a and b, the interpolation approaching analysis after TO of #14 and #17 indicated that there was no mutation in the constraint target function during 0–18 iterations in the early optimisation stage and 0–8 iterations, and the function developed according to a straight curve. A skipping mutation occurred in iterations 19 and 9, and a leap mutation occurred in 27–28 and in 15–16 until the end of the optimisation in iterations 28 and 16.

As indicated in Fig. 13c and d, the interpolation approaching analysis after TO of #18 indicated that in the early stage of optimisation, a skipping mutation occurred in 0–8, until the end of the final optimisation in 08, and a leap mutation occurred in 07–08. The approaching analysis of 80% volume optimisation indicated that from 00, intense stress changes occurred in the structure, and multiple mutations occurred in the curved line, resulting in the continuous local failure of the structure.

The conclusion of the structural finite elements and interpolation approaching analysis provides a sufficient basis, indicates the effectiveness and accuracy of the scientific fitting analysis in 4.3 and avoids a large amount of resource waste at the same time.

5. Discussion

The sustainability development assessment may be carried out based on the data analysis in Section 4. In the LCA software assessment, the unit is set as 1 kg, and 9 categories of environmental impact are used, with the software analysis results as follows. Acidification is 45.20 (kg SO_2 eq.); eutrophication is −35.10 (kg PO_4 eq.); freshwater aquatic ecotoxicity is 49.90 (kg 1,4-DB eq.); global warming (GWP100a) is 227.00(kg CO_2 eq.); human toxicity is 139.00 (kg 1,4-DB eq.); marine aquatic ecotoxicity is 108.00(kg 1,4-DB eq.); ozone layer depletion (ODP) is 0.0351 (kg CFC-11 eq.); photochemical oxidation is 62.40 (kg C_2H_4 eq.) and terrestrial ecotoxicity is 61.00 (kg 1,4-DB eq.).

Table 4
Environmental impact at the material manufacturing stage.

Name (kg)	Concrete	Asphalt concrete	Strand	Corrugated Pipe	Steel	Anchorage
Acidification	3,789,384,236.69	61,346,524.80	18,596,715.73	1,873,515.77	225,793,345.60	2,054,091.69
Eutrophication	−2,942,641,298.84	−47,638,562.40	−14,441,254.92	−1,454,876.19	−175,339,522.80	−1,595,102.17
Fresh water aquatic ecotox	4,183,413,128.56	67,725,477.60	20,530,445.02	2,068,328.25	249,271,857.20	2,267,680.87
Global warming (GWP100a)	19,030,757,117.88	308,089,848.00	93,395,010.43	9,409,028.33	1,133,962,156.00	10,315,902.95
Human toxicity	11,653,194,887.16	188,654,136.00	57,189,015.20	5,761,475.50	694,364,492.00	6,316,786.39
Marine aquatic ecotoxicity	9,054,280,919.52	146,580,192.00	44,434,630.51	4,476,542.11	539,506,224.00	4,908,006.69
Ozone layer depletion (ODP)	2,942,641.30	47,638.56	14,441.25	1,454.88	175,339.52	1,595.10
Photochemical oxidation	5,231,362,309.06	84,690,777.60	25,673,342.07	2,586,446.55	311,714,707.20	2,835,737.20
Terrestrial ecotoxicity	5,113,992,000.84	82,790,664.00	25,097,337.60	2,528,417.30	304,721,108.00	2,772,114.89

Table 5
STB design and material stage cost analysis.

Project	Name	Ratio	Calculation method	Quantity (CNY)
1	Direct fee	/	Material quantity × unit price	64,728,088.08
2	Insurance	3%	1 × 2	1,941,842.64
3	Completion and environmental protection fees	1,500,000	Fixed costs	1,500,000.00
4	Safety production fee	1.5%	1 × 4	970,921.32
5	Management information fee	200,000	Fixed costs	200,000.00
6	Temporary road, land occupation	4.41%	1 × 6	265,385.16
7	Temporary power supply and communication	0.16%	1 × 7	103,564.94
8	Water supply and sewage facilities	0.08%	1 × 8	51,782.47
9	Standard chemical field construction	0.42%	1 × 9	271,857.97
10	Provisional amount	5%	(1 + 2 + 3 + 4 + 5 + 6 + 7 + 8 + 9) × 10	73,535,114.71
Estimated total price	/	/	/	77,036,786.84

5.1. Environmental impact

Table 4 offers the environmental impact data of the STB design and material stages. The emission ranking is as follows: Global warming (GWP100a) > Human toxicity > Marine aquatic ecotoxicity > Photochemical oxidation > Terrestrial ecotoxicity > Fresh water aquatic ecotoxicity. The emission load is 20,585,929,063.59 > 12,605,480,792.24 > 9,794,186,514.84 > 5,658,863,319.68 > 5,531,901,642.64 > 4,525,276,917.50 kg, respectively.

5.2. Economic

The direct cost is calculated based on the project quantities in Table 1. Since a bridge built in China in 2009 is selected as the case, the economic cost is analysed by applying the highway ratio in China. Total expenses incurred in that year were 77,036,786.84 CNY, including the direct costs of 64,728,088.08 CNY (Table 5), accounting for 84.02% of the total expenses.

In accordance with eq. (7), the total economic cost = $\sum_{t=\text{Design}}^{\text{Material manufacturing}} C_T = 77036786.84 + \frac{77036786.84}{(1+0.03086)^{2021-2009}} = 121{,}613{,}061.678$ CNY (the interest rate for commercial general loans over five years is 4.90%) [51].

Conclusion: The bridge has been in operation for 12 years (until 2021) with a total cost of 121,613,061.678 CNY.

Table 7
Analysis data of the reduced impact after STB optimisation.

Location	LCA(Kg)	LCC (CNY)	SIA (Med risk hours)
#14	752,375.3028	3,844,768.65	1,089,946.79
#17	698,800.2591	3,570,990.86	1,012,334.00
#18	767,340.498	3,921,243.40	1,111,626.49

5.3. Social impact

The conclusions given in Table 6 were obtained through the analysis using OpenLCA1.10.3 software. 34,475,875.85 Med risk hours were generated, including 34.17% of corruption and 22.8% of sanitation coverage.

5.4. Analysis after optimisation

In accordance with the analysis conclusion in 4.5, the reduction in concrete used for #14, #17 and #18 after STB TO is 1144.41 m^3, 1062.92 m^3 and 1167.17 m^3, respectively, accounting for 3.16%, 2.94% and 3.22% of the total amount of concrete in the existing components, respectively. The reduced amount after optimisation is shown in Table 7.

5.5. Multifactor approximation analysis

The influencing factors of LCA, LCC and SIA are marked as *x*, *y* and z matrices, and the *x*, *y* and *z* influence equations are fitted using the programmed algorithm ④:

In Fig. 14a and b the influence equation and curve graph after analysis are given.

Linear model Poly22:

$$f(x,y) = z = p00 + p10 \times x + p01 \times y + p20 \times x^2 + p11 \times x \times y + p02 \times y^2 \quad (10)$$

Table 6
STB social impact analysis data.

Project division phase	STB (Med risk hours)				
	Fatal accidents	International migrant workers	Youth illiteracy	Corruption	Sanitation coverage
Design stage	1,567,119.534	1,370,010.833	909,386.0939	3,053,740.957	2,037,932.615
Material manufacturing stage	4,477,484.382	3,914,316.667	2,598,245.983	8,724,974.164	5,822,664.616

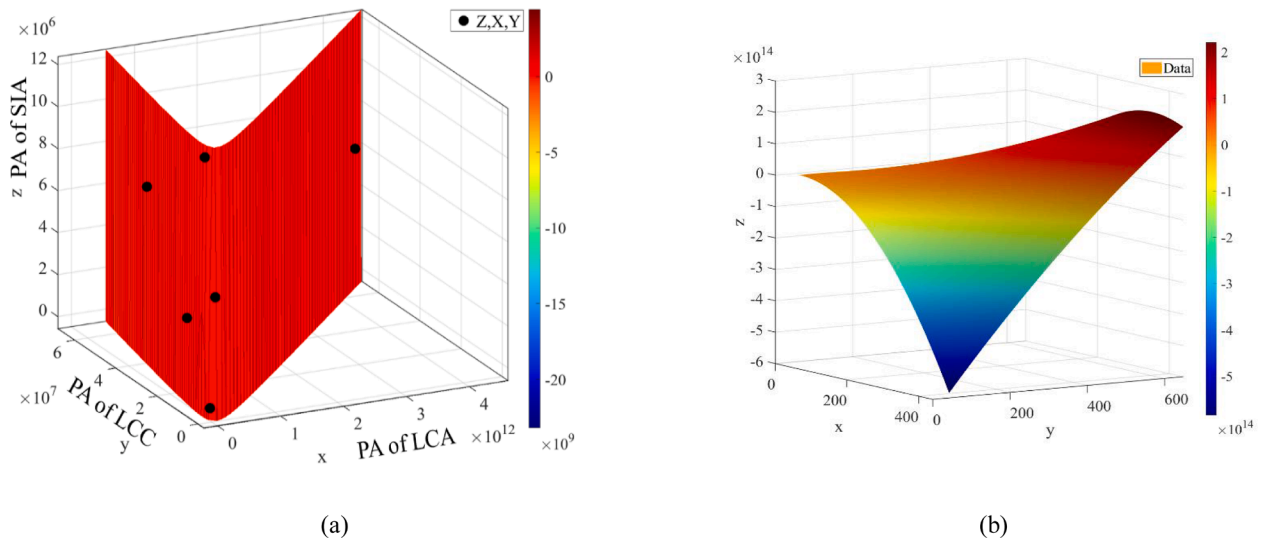

Fig. 14. Interpolated fitting image and optimized equation surface image (PA = polynomial approximation): (a) Interpolated fitting; (b) Equation surface.

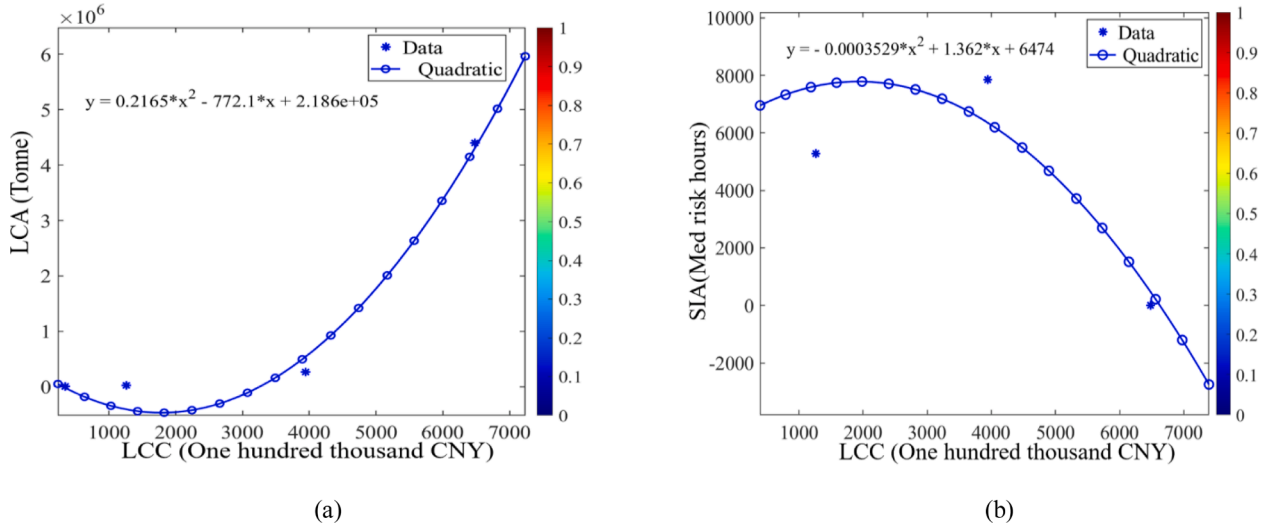

Fig. 15. The influence equation: (a) The influence equation after fitting x and y; (b) The influence equation after fitting y and z.

Standardized processing of x and y data: The x index is within the range of 7.935e + 11 and 1.77e + 12, and a comprehensive evaluation is performed to obtain the standardized data of x. The y index is within the range of 2.027e + 07 and std 2.633e + 07, and a comprehensive evaluation is performed to obtain the standardized data of y. After × and y are standardized, the coefficients of the fitting equation are obtained: $p00 = 5.885e + 08$, $p10 = 1.079e + 08$, $p01 = 1.111e + 09$, $p20 = -3.366e + 09$, $p11 = 3.67e + 09$, $p02 = -4.758e + 08$.

The influence equations of x and y, y and z are fitted, respectively, in accordance with the programmed algorithms ② and ③.

Fig.15a reflects the influence analysis equation and curve graph:

$$Y = 0.2165 \times x^2 + 772.1 \times x + 2.186e + 05 \quad (11)$$

Fig.15b shows the influence analysis equation and curve graph:

$$Y = -0.0003529 \times x^2 + 1.362 \times x + 6474 \quad (12)$$

5.6. Regional environmental impact analysis

Economic growth has a nonlinear and non-monotonic correlation with environmental disruption, which causes considerable losses to the regional economy. Accurately quantifying the causal relationship between the assessment and utilization of economic development, the environment and natural resources are necessary scientific contributions [52].

Table 8
Statistics related to the amount of investment in the economy, construction, and society in Huzhou City and Zhejiang Province [53].

Years (Billion CNY)	Social investment in fixed assets		Infrastructure investment	
	Huzhou	Zhejiang	Huzhou	Zhejiang
2009	636.19	10,742.32	141.16	1,908.00
2010	719.98	12,376.04	120.74	2,061.50
2011	804.67	14,290.00	144.21	2,295.30
2012	970.73	60,980.00	166.71	3,963.00
2013	1,070.05	73,322.00	219.49	4,718.09
2014	1,242.92	84,266.00	260.73	5,741.56
2015	1,402.64	89,088.00	324.30	7,417.75
2016	1,592.18	97,729.00	466.70	9,365.48
2017	1,730.98	109,016.00	576.23	10,173.25
2018	1,838.30	116,756.10	611.96	10,956.59
2019	2,047.86	128,548.50	681.72	11,811.20

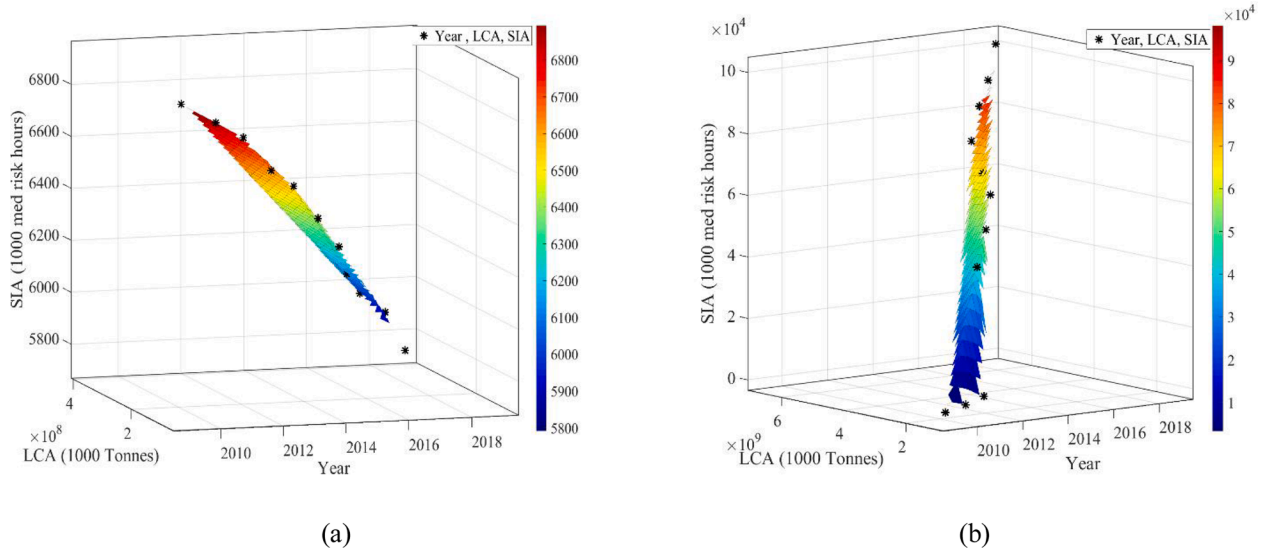

Fig. 16. Calculation data verification: (a) Huzhou; (b) Zhejiang.

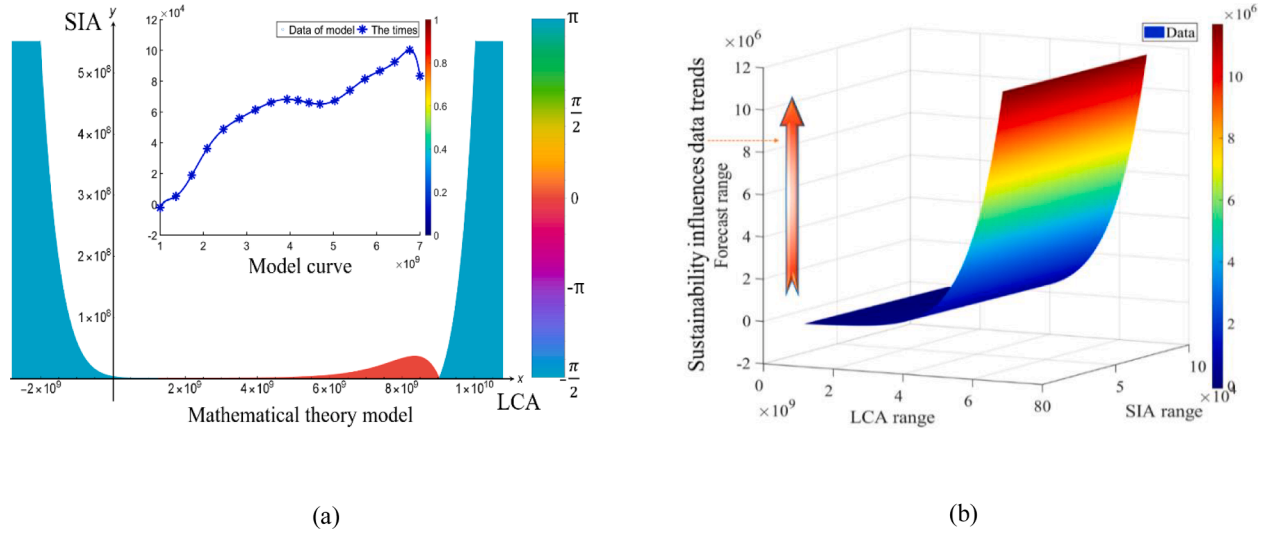

Fig. 17. Analysis: (a) Regional model analysis; (b) Regional sustainable development data forecast.

5.6.1. Infrastructure and LCA linear interpolation measurement

The programmed algorithm ② and Table 8 are used to calculate the LCA data from 2009 to 2019 (as shown in Fig. 16a):

y = 0.2165 × x^2-772.1×x +(2.186e + 05); % Regional LCA and Infrastructure Impact Equation.

yi nearest = interp1(x, y, xi,' nearest').

5.6.2. Infrastructure and SIA linear interpolation measurement

The programmed algorithm ② and Table 8 are used to calculate the SIA data from 2009 to 2019 (as shown in Fig. 16b): y = -0.0003529×x^2 + 1.362×x + 6474; % Regional SIA and infrastructure impact equation.

5.6.3. Regional sustainable development model equations

After analysing the fitting accuracy of the scientific algorithm for the sustainable development data of Hu Zhou from 2009 to 2020, it is concluded that linear interpolation can be used; f(x, y) = piecewise linear surface computed from p (Fig. 16a); the x index was within the range of 2014 and 3.317, and a comprehensive evaluation was performed to obtain the standardized data of x. The y index was within the range of 1.94e + 08 and std 1.207e + 08, and a comprehensive evaluation was performed to obtain the standardized data of y. The goodness of fit was SSE = 0; the data forecast is accurate.

After analysing the fitting accuracy of the scientific algorithm for the sustainable development data of Zhe Jiang from 2009 to 2020, it is concluded that linear interpolation can be used, f(x, y) = piecewise linear surface computed from p (Fig. 16b); the x index was within the range of 2014 and 3.317, and a comprehensive evaluation was performed to obtain the standardized data of x. The y index is within the range of 3.685e + 09 and std 2.148e + 09, and a comprehensive evaluation was performed to obtain the standardized data of y. The goodness of fit was SSE = 0; the data forecast is accurate.

The program algorithm ②③④ was used to predict the impact of regional infrastructure and sustainable development. The scientific algorithm model obtains the Zhejiang Province (2009–2020) sustainable impact assessment data as:

Database of LCA: [1098252700 1,186,638,000 1,321,260,040 2,281,521,700 2,716,302,522 3,305,616,548 4,270,766,750 5,392,269,684 5,857,383,650 6,308,430,822 6800515260].

Database of SIA: [1536.20836 2901.18142 4500.295 43509.79 53821.531 62965.243 66994.024 74213.5795 83643.868 90110.638

99963.27175].

Establish regional mathematical theory model (Fig. 17a). Using polynomial fitting for the model, check the accuracy of the curve equation, goodness of fit R2 = 1, RMSE = 1.864e-09 (the root mean square standard deviation is the smallest), indicating that the fitting model is successful. Sustainable development and time assessment influence equation (Fig. 17b).

In $F(x, y)$, x is the calculated value of 5.6.1 and 5.6.2 linear interpolation, and y is the value of sustainable development impact assessment.

6. Conclusions

Structural construction has had increasingly severe impacts on sustainable development in the construction industry. How to research and analyse this accurately and effectively is the responsibility and obligation of every scientific researcher. The present paper has indicated the key controlling factors related to the sustainable development of bridges. It describes how to effectively apply scientific analysis methods to achieve optimization objectives through the systematic analysis of bridge sustainability.

The present research began with modeling the three pillars of the environment, economy, and society and the programming of a scientific algorithm. Then, we analysed the case study bridge in detail, from the initial sustainable development assessment to the distribution optimization of components and extended the analysis of a single bridge structure to study regional infrastructure and economic development. The research used five software packages and compiled more than ten scientific algorithms (the drawing algorithm program is not listed), which effectively ran through the whole research work and led to conclusions. The optimization of the total component concrete by 9.32% was performed, and the 11-year sustainable development data in the region and the regional future sustainable development assessment influence equation were obtained.

The data and methods obtained from the present research are suitable for studying similar components in other areas and can be used as a reference for further research in this field. The sustainable development assessment equation established by this research is suitable for data assessment in all countries globally; it will provide an essential theoretical reference for the global future sustainable development assessment. Follow-up research will focus on the following aspects: the influence of sustainable development of regional structures on the global climate, the optimization design of flexible topology for the regional construction industry, and the relationship between the implementation of *trans*-regional sustainable development strategy structural optimization.

Declaration of Competing Interest

The authors declare that they have no known competing financial interests or personal relationships that could have appeared to influence the work reported in this paper.

Acknowledgements

The authors gratefully acknowledge the funding received from the following research projects: Grant PID2020-117056RB-100 founded by MCIN/AEI/10.13039/501100011033 and by “ERDF A way of making Europe”. The authors thank Dr. Debra Westall (UPV) for revising the manuscript for publication.

References

[1] Nations U, of Economic D, Affairs S, Division P. World Urbanization Prospects The 2018 Revision. 2018. https://population.un.org/wup/Publications/Files/WUP2018-Report.pdf. (Accessed 8 May 2022).
[2] Tukker A, Bulavskaya T, Giljum S, De Koning A, Lutter S, Simas M, et al. The Global Resource Footprint of Nations The Global Resource Footprint of Nations Content. 2014. http://www.truthstudio.com/content/CREEA_Global_Resource_Footprint_of_Nations.pdf. (Accessed 8 May 2022).
[3] Li Q, Long R, Chen H, Chen F, Wang J. Visualized analysis of global green buildings: development, barriers and future directions. J Clean Prod 2020;245:118775. https://doi.org/10.1016/j.jclepro.2019.118775.
[4] Olawumi TO, Chan DWM. Critical success factors for implementing building information modeling and sustainability practices in construction projects: a Delphi survey. Sustain Dev 2019;27:587–602. https://doi.org/10.1002/sd.1925.
[5] Elsevier Scopus, Citation database 2021. https://www.elsevier.com/solutions/scopus. (Accessed 8 May 2022).
[6] Chen C. Science mapping: a systematic review of the literature. J Data Inf Sci 2017;2:1–40. https://doi.org/10.1515/jdis-2017-0006.
[7] UNFCCC, Off-grid and decentralized energy solutions for smart energy and water use in the agrifood chain. 2019. https://unfccc.int/documents/208414. (Accessed 8 May 2022).
[8] C40 Cities Climate Leadership Group, Arup, University of Leeds, The future of urban consumption in a 1.5°C world. Arup & University of Leeds. Leeds, United Kingdom 2019. https://www.c40knowledgehub.org/s/article/The-future-of-urban-consumption-in-a-1-5-C-world?language=en_US. (Accessed 8 May 2022).
[9] García-Segura T, Penadés-Plà V, Yepes V. Sustainable bridge design by metamodel-assisted multi-objective optimization and decision-making under uncertainty. J Clean Prod 2018;202:904–15. https://doi.org/10.1016/j.jclepro.2018.08.177.
[10] Sigmund O, Maute K. Topology optimization approaches: a comparative review. Struct Multidiscip Optim 2013;48(6):1031–55.
[11] Zhang W, Kang Z. Robust shape and topology optimization considering geometric uncertainties with stochastic level set perturbation. Int J Numer Methods Eng 2017;110:31–56. https://doi.org/10.1002/nme.5344.
[12] Luo Y, Zhou M, Wang MY, Deng Z. Reliability based topology optimization for continuum structures with local failure constraints. Comput Struct 2014;143:73–84. https://doi.org/10.1016/j.compstruc.2014.07.009.
[13] Amir O, Sigmund O. On reducing computational effort in topology optimization: How far can we go? Struct Multidiscip Optim 2011;44:25–9. https://doi.org/10.1007/s00158-010-0586-7.
[14] Luo F, Guo Y, Yao M, Cai W, Wang M, Wei W. Carbon emissions and driving forces of China’s power sector: input-output model based on the disaggregated power sector. J Clean Prod 2020;268:121925. https://doi.org/10.1016/j.jclepro.2020.121925.
[15] Deng H, To AC. Linear and nonlinear topology optimization design with projection-based ground structure method (P-GSM). Int J Numer Methods Eng 2020;121:2437–61. https://doi.org/10.1002/nme.6314.
[16] Li Y, Li X, Li M, Zhu Y, Zhu B, Jiang C. Lagrangian-Eulerian multi-density topology optimization with the material point method. Int J Numer Methods Eng 2021;122:3400–24. https://doi.org/10.1002/nme.6668.
[17] Dubey S, Mittal R, Lauritzen PH. A flux-form conservative semi-Lagrangian multitracer transport scheme (FF-CSLAM) for icosahedral-hexagonal grids. J Adv Model Earth Syst 2014;6:332–56. https://doi.org/10.1002/2013MS000259.
[18] Ferrer A. SIMP-ALL: a generalized SIMP method based on the topological derivative concept. Int J Numer Methods Eng 2019;120:361–81. https://doi.org/10.1002/nme.6140.
[19] Li J, Liu W, Bao Y. Genetic algorithm for seismic topology optimization of lifeline network systems. Earthq Eng Struct Dyn 2008;37:1295–312. https://doi.org/10.1002/eqe.815.
[20] Zhou Z, Alcalá J, Yepes V. Environmental, economic and social impact assessment: study of bridges in China’s five major economic regions. Int J Environ Res Public Health 2020;18:122. https://doi.org/10.3390/ijerph18010122.
[21] Statistics, Z.P.B. of. Statistical Yearly Sign. Stat. Zhejiang Prov. Bur, 2021. http://tjj.zj.gov.cn/col/col1525563 /index.html. (Accessed 8 May 2022).
[22] Ciroth, A., Eisfeldt, F., PSILCA database, 2016. https://psilca.net/. (Accessed 8 May 2022).
[23] Bendsøe MP, Sigmund O. Material interpolation schemes in topology optimization. Arch Appl Mech (Ingenieur Arch 1999;69:635–54. https://doi.org/10.1007/s004190050248.
[24] Zhang XS, Paulino GH, Ramos AS. Multimaterial topology optimization with multiple volume constraints: combining the ZPR update with a ground-structure algorithm to select a single material per overlapping set. Int J Numer Methods Eng 2018;114(10):1053–73.
[25] Fu Z, Wang C. Robust topology optimization of periodic structures under uncertain loading. Beijing Hangkong Hangtian Daxue Xuebao/Journal Beijing Univ Aeronaut Astronaut 2017;43:747–53. https://doi.org/10.13700/j.bh.1001-5965.2016.0822.
[26] Forman P, Gaganelis G, Mark P. Optimierungsgestützt entwerfen und bemessen. Bautechnik 2020;97:697–707. https://doi.org/10.1002/bate.202000054.
[27] Xu X, Fan W, Xie X. Hybrid stress quadrilateral finite element approximation for stochastic plane elasticity equations. Int J Numer Methods Eng 2017;109:1418–38. https://doi.org/10.1002/nme.5333.

[28] Lehtonen M. The environmental–social interface of sustainable development: capabilities, social capital, institutions. Ecol Econ 2004;49:199–214. https://doi.org/10.1016/j.ecolecon.2004.03.019.
[29] Ballet J, Bazin D, Mahieu F. A policy framework for social sustainability: Social cohesion, equity and safety. Sustain Dev 2020;28:1388–94. https://doi.org/10.1002/sd.2092.
[30] ISO. ISO14044:2006/AMD2:2020 Environmental management-Life cycle assessment-Requirements and guidelines. ISO, 2020. https://www.iso.org/standard/76122.html.
[31] Penadés-Plà V, Martí JV, García-Segura T, Yepes V. Life-cycle assessment: a comparison between two optimal post-tensioned concrete box-girder road bridges. Sustainability 2017;9(10):1864.
[32] Zhou Z, Alcalá J, Yepes V. Bridge carbon emissions and driving factors based on a life-cycle assessment case study: cable-stayed bridge over Hun He River in Liaoning, China. Int J Environ Res Public Health 2020;17:5953. https://doi.org/10.3390/ijerph17165953.
[33] Goto M, Sueyoshi T. Sustainable development and corporate social responsibility in Japanese manufacturing companies. Sustain Dev 2020;28:844–56. https://doi.org/10.1002/sd.2035.
[34] Hao Y, Wang Y, Wu Q, Sun S, Wang W, Cui M. What affects residents' participation in the circular economy for sustainable development? Evidence from China. Sustain Dev 2020;28:1251–68. https://doi.org/10.1002/sd.2074.
[35] Leipold S, Petit-Boix A. The circular economy and the bio-based sector - Perspectives of European and German stakeholders. J Clean Prod 2018;201:1125–37. https://doi.org/10.1016/j.jclepro.2018.08.019.
[36] European Commission. Farm to fork strategy for sustainable food. Eur. Comm,2019. https://ec.europa.eu/food/farm2fork_en. (Accessed 8 May 2022).
[37] Elmagrhi MH, Ntim CG, Elamer AA, Zhang Q. A study of environmental policies and regulations, governance structures, and environmental performance: the role of female directors. Bus Strateg Environ 2019;28:206–20. https://doi.org/10.1002/bse.2250.
[38] Shahab Y, Ntim CG, Chen Y, Ullah F, Li H, Ye Z. Chief executive officer attributes, sustainable performance, environmental performance, and environmental reporting: New insights from upper echelons perspective. Bus Strateg Environ 2020;29:1–16. https://doi.org/10.1002/bse.2345.
[39] Lu W, Ye M, Chau KW, Flanagan R. The paradoxical nexus between corporate social responsibility and sustainable financial performance: evidence from the international construction business. Corp Soc Responsib Environ Manag 2018;25:844–52. https://doi.org/10.1002/csr.1501.
[40] Paya-Zaforteza I, Yepes V, González-Vidosa F, Hospitaler A. On the Weibull cost estimation of building frames designed by simulated annealing. Meccanica 2010;45:693–704. https://doi.org/10.1007/s11012-010-9285-0.
[41] Sierra LA, Pellicer E, Yepes V. Method for estimating the social sustainability of infrastructure projects. Environ Impact Assess Rev 2017;65:41–53. https://doi.org/10.1016/j.eiar.2017.02.004.
[42] Benoît C, Mazijn B. Guidelines for Social Life Cycle Assessment of Products; UNEP/SETAC Life Cycle Initiative, Sustainable Product and Consumption Branch: Paris, France, 15, ISBN 9789280730210, 2009. https://www.unep.org/resources/report/guidelines-social-life-cycle-assessment-products. (Accessed 8 May 2022).
[43] Rangel RL, Martha LF. LESM—An object-oriented MATLAB program for structural analysis of linear element models. Comput Appl Eng Educ 2019;27:553–71. https://doi.org/10.1002/cae.22097.
[44] China, M. of T. of the P.R. of, 2015. "General Code for Design of Highway Bridges and Culverts" (JTG D60-2015)-Traffic Books-Ministry of Transport of the People's Republic of China. Minist. Transp. People's Repub. China,2021. https://www.mot.gov.cn/jiaotongtushu/201512/t20151229_1967723.html. (Accessed 8 May 2022).
[45] Li Y, Cao S, Jing D. Analytical compressive stress-strain model for concrete confined with high-strength multiple-tied-spiral transverse reinforcement. Struct Des Tall Spec Build 2018;27:e1416. https://doi.org/10.1002/tal.1416.
[46] Zhou Z, Alcalá J, Kripka M, Yepes V. Life cycle assessment of bridges using Bayesian networks and fuzzy mathematics. Appl Sci 2021;11:4916. https://doi.org/10.3390/app11114916.
[47] Cole DJ, McCrea RS. Parameter redundancy in discrete state-space and integrated models. Biom J 2016;58:1071–90. https://doi.org/10.1002/bimj.201400239.
[48] Yepes V, Martí JV, García-Segura T. Cost and CO_2 emission optimization of precast-prestressed concrete U-beam road bridges by a hybrid glowworm swarm algorithm. Autom Constr 2015;49:123–34. https://doi.org/10.1016/j.autcon.2014.10.013.
[49] Liang C, Xiao J, Wang Y, Wang C, Mei S. Relationship between internal viscous damping and stiffness of concrete material and structure. Struct Concr 2021;22(3):1410–28.
[50] Cai J, Wang C, Fu Z. Robust concurrent topology optimization of multiscale structure under single or multiple uncertain load cases. Int J Numer Methods Eng 2020;121:1456–83. https://doi.org/10.1002/nme.6275.
[51] Jin X, Song FM, Wang Y, Zhong Y. Interest rate pass-through in a dual-track system: evidence from China. China World Econ 2014;22:21–39. https://doi.org/10.1111/j.1749-124X.2014.12073.x.
[52] Coxhead I. Development and the environment in Asia. Asia Pac Econ Lit 2003;17:22–54. https://doi.org/10.1111/1467-8411.t01-1-00013.
[53] Statistics ZPB of. Statistical Yearly Sign. Stat Zhejiang Prov Bur 2021:1–17. http://tjj.zj.gov.cn/col/col1525563/index.html. (Accessed 8 May 2022).